The Prospect of a kW-Class, Multi-TW, ps Laser

Contact *Klaus.ertel@stfc.ac.uk*

K. Ertel, S. Banerjee, A. Boyle, I. O. Musgrave, W. Shaikh, S. Tomlinson, M. De Vido, T. B. Winstone, A. S. Wyatt, C. B. Edwards, C. Hernandez-Gomez, J. L. Collier

STFC Rutherford Appleton Laboratory, Central Laser Facility, Chilton, Didcot, OX11 0QX, UK

Abstract

We explore how DiPOLE-type laser systems, based on cryo-cooled, diode pumped, multi-slab Yb:YAG amplifier technology, can be adapted for direct-CPA ps-pulse generation, opening up the possibility of producing pulses with 10s of TW of peak power, 10s of J of energy, at the kW average power level, without having to resort to more complex and less efficient schemes like OPCPA or Ti:Sapphire amplifier chains. Initial calculations indicate that the narrow gain-bandwidth of cryo-cooled Yb:YAG is challenging in terms of stretching and recompression of the laser pulses, but nonetheless should allow the generation of 2 ps pulses at nearly the same energy and at the same repetition rate as in ns mode.

1. Introduction

The DiPOLE platform, developed at the CLF and based on a diode-pumped, cryo-cooled, multi-slab Yb:YAG amplifier architecture, is designed to deliver few-ns pulses at the same pulse energies (ultimately up to the kJ level) as conventional flashlamp-pumped Nd:glass laser systems, but at a much higher repetition rate in the multi-Hz range, and at a much higher efficiency. The performance demonstrated with existing DiPOLE-type systems include generation 100 J pulses of 10 ns duration at 10 Hz repetition rate, making it the first laser, to our knowledge, that has produced such high-energy ns pulses at such high average power [1]. Frequency-doubling of the 1030 nm output radiation at efficiencies exceeding 80 % has also been shown [2].

This makes DiPOLE ideally suited to pump fs-amplifiers (Ti:sapphire or OPCPA) for the production of multi-Hz PW pulses, which have a multitude of uses, in particular for the realisation of secondary sources, such as laser driven particle, X-ray, or gamma sources [3].

While Ti:sapphire and OPCPA systems deliver extremely short, high peak power pulses, owing to their large gain-bandwidth, their overall efficiency is rather low, and their complexity large, both as a result of the multiple conversion stages involved, where typically the output of a 1 µm ns laser is first frequency doubled and then used to pump amplifiers for the near-IR ultrashort pulses.

An alternative is presented by the direct CPA approach, using laser amplifiers which can be pumped directly by laser diodes, and which offer enough bandwidth such that stretched ultrashort pulses can be directly amplified and then re-compressed to the ps range. Such lasers promise increased efficiency, especially if diode pumping is used, and reduced complexity, while the pulse durations and peak powers they offer are still suitable for a number of applications.

We have therefore started to explore if and how the DiPOLE 100 laser could be converted into a CPA system, with minimum changes to the original set-up in order to preserve the capability to generate arbitrarily shaped ns-pulses of variable length.

A block diagram of the DiPOLE 100 system is shown in Figure **1**. The amplifiers that would be used for both CPA and ns operation are: PA1, a regenerative amplifier based on Yb-doped CaF2, with an output energy of few mJ; PA2, a multi-pass amplifier with Yb:YAG at room temperature as gain medium, producing 100 mJ; MA1, a cryo-cooled, Yb:YAG multi-pass amplifier producing up to 10 J; and MA2, a scaled-up version of MA1, producing up to 100 J.

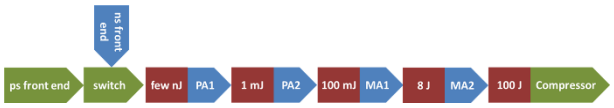

Figure 1: Main components of DiPOLE 100. Blue: original components of ns laser; green: additional components for CPA operation; red: approximate pulse energy at input of component; PA: pre-amplifier; MA: main amplifier.

In CPA mode, the ns front-end is replaced by a ps front-end, consisting of a mode-locked oscillator and a stretcher. A grating compressor is added at the end of the chain.

2. Spectral and gain modelling

The DiPOLE architecture relies on cryo-cooled main amplifier stages to achieve efficient energy extraction at moderate fluence levels. However, the gain bandwidth of Yb:YAG significantly decreases with temperature, which poses a major challenge for CPA operation. Sufficient spectral width of the amplified pulses is required to achieve a short compressed pulse duration and, even more importantly, to achieve a sufficiently long *stretched* pulse duration in order to avoid optical damage and detrimental nonlinear effects in the amplifier chain.

Figure 2 illustrates the trade-off associated with cryo-cooled Yb:YAG amplifiers: the width of the fluorescence (or gain) spectrum decreases with decreasing temperature, whilst the emission cross section increases, with the product of the two remaining approximately constant.

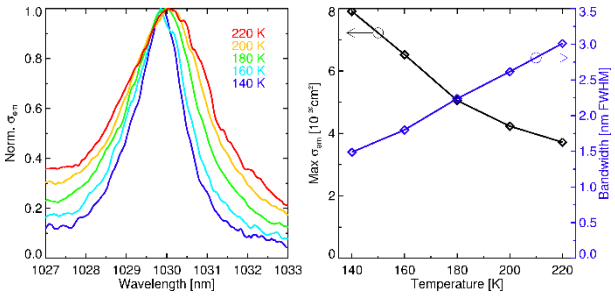

Figure 2: Normalised fluorescence spectra of Yb:YAG at temperatures between 140K and 220K (left panel, from [5]); right panel, maximum emission cross section and width of Yb:YAG fluorescence at different temperatures.

To simulate amplification of stretched broadband pulses, an existing numerical amplifier model, described in [4], has been adapted to include spectrally resolved emission cross sections, as shown in Fig. 2. The model simulates the amplification of a chirped pulse in the temporal domain, with a certain wavelength

being associated with each time interval within the pulse. The pulses were assumed to be linearly stretched in time, with a stretch factor of 2 ns/nm. This stretch factor should yield sufficiently long stretched pulses at the output of the amplifier chain. The resulting temporal and spectral shapes, obtained after optimizing some parameters, are shown in Figure **3**.

The calculated pulse energies after the individual stages are 1 mJ, 100 mJ, 8 J and 100 J, respectively. The cumulated B-Integral is 1.6 rad and the effective bandwidth (derived from the standard deviation of the spectral distribution and equivalent to the FWHM of a Gaussian curve) is 0.85 nm, corresponding to a transform limited pulse duration of about 2 ps.

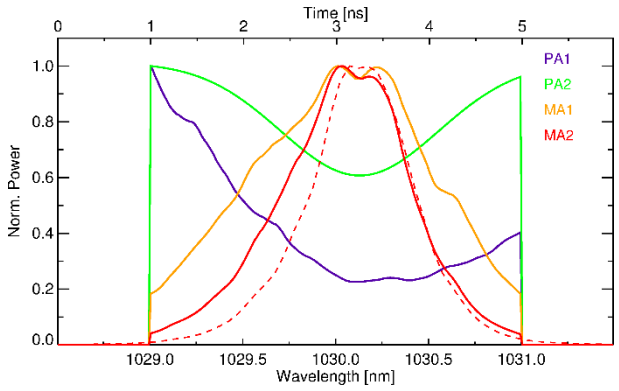

Figure 3: Simulated pulse/spectral shapes after different amplifier stages. Dashed line: result for a non-optimised input-shape, a 3 nm wide top-hat.

The spectra shown in Figure **3** are the result of some optimisation which includes the following elements:

- Restricting the width of the input spectrum to a range where non-negligible gain is experienced in the last amplifier stage. Spectral components outside this window would unnecessarily extract energy from the earlier stages, while being lost in the latter stages, lowering the overall efficiency. In the scenario presented here the width of the input spectrum was restricted to 2 nm.
- Active shaping of the input spectrum, using a tuneable filter in the front-end. A desired shape with a central dip was prescribed for the output of PA2. The required input shape from the front-end was calculated using an iterative algorithm. It is assumed that PA1 does not introduce significant spectral distortion due to the large bandwidth of the CaF_2 gain medium.
- Operating the cryo-cooled amplifiers at a higher than usual temperature and compensating for the reduced gain by higher pump energy (within the capabilities of the existing pump sources). The temperatures chosen for PA1 and PA2 were 200 K and 180 K, respectively, instead of the usual 150 K.

3. Pulse stretching, compression, and dispersion management

The results shown in the previous section indicate that a stretch factor of 2 ns/nm is required to keep the peak intensity of the stretched pulse within tolerable levels. While novel stretching schemes such as chirped fibre Bragg gratings are being investigated, it is not yet clear whether the required stretch factor and compressibility can be achieved this way. Therefore a conventional, grating-based Offner stretcher has been designed, together with a grating compressor whose dispersion is matched to the stretcher.

Ray-tracing diagrams of stretcher and compressor are shown Figure **4** and Figure **5**, respectively. The grating line density is 1740 mm^{-1} and the incident angle is 56 °, 11 ° away from the Littrow angle. The stretcher has a length of about 5 m and is a double-pass design where the beam passes the grating a total of eight times. Due to the limited spectral acceptance window of 3 nm (which could be further reduced down to 2 nm), the optics are relatively small, with the grating being the largest component, needing to accommodate a beam footprint of 320x60 mm^2.

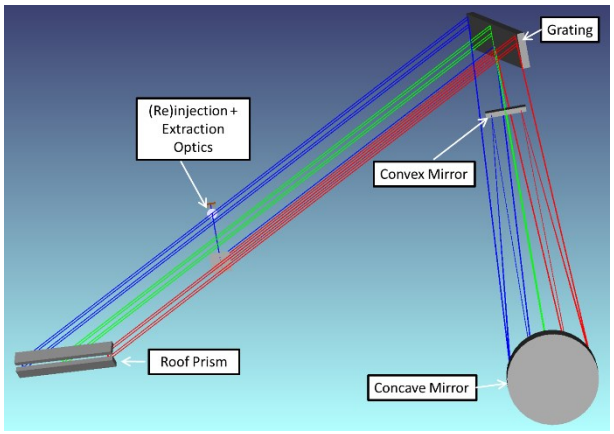

Figure 4: Ray-tracing model of an Offner stretcher using a 1740l/mm grating to achieve a chirp rate of 2ns/nm.

The compressor is a folded double-pass design with two large gratings with incoming and outgoing beams sitting above each other. For a transmission of 70%, 70 J compressed pulse energy would be obtained. The footprint of this arrangement is 4.5x2.5 m^2. The largest optic in the system is the second grating with a size of 700x460 mm^2, resulting in a spectral acceptance window of 2 nm, commensurate with the spectra shown in Fig. 2.

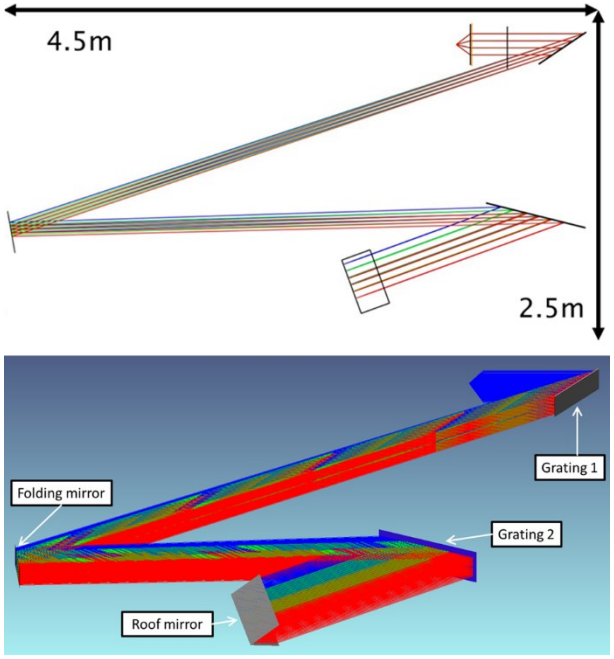

Figure 5: Ray-tracing model for the grating compressor - top view (upper panel) and isometric view (lower panel).

The beam size during compression is 200x200 mm^2, yielding a fluence of 250 mJ/cm^2 (at normal incidence) which would be suitable for gold-coated gratings. However, the high average power, which would result in a significant thermal load, and the large off-Littrow angle, which would result in a reduced diffraction efficiency in gold coated gratings, would make the use of multi-layer dielectric (MLD) gratings preferable. Currently though, the maximum safe long-term operating fluence of MLD gratings, especially under high repetition rate operation is still uncertain and is likely to lie well below the 1 J/cm^2 level usually quoted by manufacturers. One demonstrated high-energy, high repetition rate laser with an

MLD grating compressor uses a 4 cm beam diameter at a pulse energy of 1.5 J (equivalent to 120 mJ/cm^2), albeit in a more Gaussian-like beam [6].

To achieve re-compression of the stretched pulses to near the Fourier limit, grating separation in stretcher and compressor needs to be matched to within in a fraction of a millimetre and grating angles need to be controlled to within few microradians. The dispersion of optical components on the other hand, i.e. bulk dispersion and especially coating dispersion is almost negligible. For example 15 m of fused silica (in the form of optical fibres in the front-end) would only result in a lengthening of the compressed pulse by about 1 ps and can easily be compensated by a small change in grating distance. Higher order dispersion terms introduced by optical components, other than group velocity dispersion, which would require additional degrees of freedom for compensation, are of no concern.

6. Layout

We have developed a conceptual design that shows how the DiPOLE 100 Laser, the ps-frontend (based on a grating stretcher), the compressor including short-pulse diagnostics, and a beam transport system, could be accommodated in a laboratory.

This concept is shown in Fig. 6. A layout where all major components are arranged in a line would require a laboratory about 30 m in length. The beam is generated in the front-end, located near the middle of the room, and then makes its way through the various amplifier stages, towards the far-end of the room. The beam is then sent back to the near end of the room by means of an expanding vacuum telescope which increases the beam width from 75 mm at the output of the amplifier chain, to 200 mm, required for injection into the compressor. Using a very long expanding telescope minimises the pulse-front distortion that is caused by the chromatic distortion in the large-aperture output lens [7].

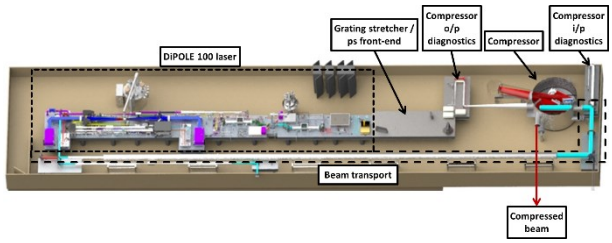

Figure 6: possible layout of laboratory accommodating DiPOLE 100 laser and CPA add-ons.

A mechanical concept for the large grating compressor, which has to operate in vacuum, was also developed. The simplest solution would be to house the compressor optics (see Fig. 5) in a rectangular chamber. The high forces acting on the chamber walls would however require strengthening those by extensive external support structures, leading to a design that would require excessive amounts of material and the external volume (and resulting requirements regarding space and access routes) would be substantially bigger than the internal volume.

The fact that most optics are located on one side opens the possibility to adopt a split-chamber design, shown in Fig. 7. All optics, except the folding mirror, are located inside a cylindrical tank, which is a much more favourable geometry with regards to mechanical strength, with the folding mirror located in a smaller satellite chamber which is connected the main tank by a pipe that accommodates the beams going to the folding mirror. A challenge is to ensure that all optics maintain their position, and more importantly, angular orientation, within tight limits, and that those positions must remain stable during pump-down and let-up of the vacuum. This is usually achieved by mounting the optics on a structure that has its own floor supports and is decoupled from the vacuum chamber by the means of flexible bellows.

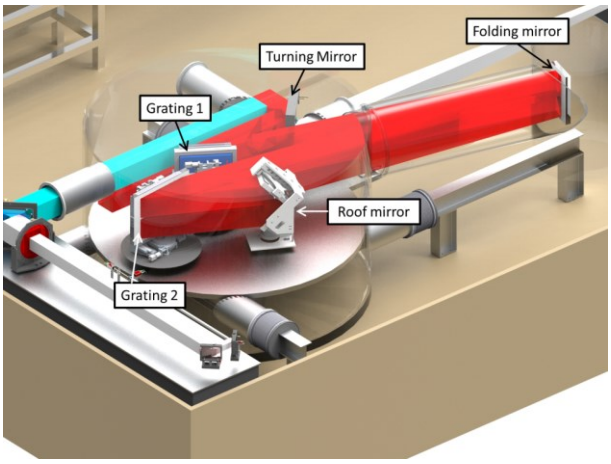

Figure 7: Compressor optics inside vacuum chamber.

7. Conclusion

We have shown that the DiPOLE platform can be adapted to direct CPA operation and has the potential to produce multi-TW pulses at unprecedented pulse energies and average powers. Required for this are careful optimisation of the amplified spectral bandwidth, stretcher and compressor systems with very high dispersion (but limited spectral throughput), and compressor gratings that are not adversely affected by kW average powers.

References

[1] Paul Mason, Martin Divoký, Klaus Ertel, Jan Pilař, Thomas Butcher, Martin Hanuš, Saumyabrata Banerjee, Jonathan Phillips, Jodie Smith, Mariastefania De Vido, Antonio Lucianetti, Cristina Hernandez-Gomez, Chris Edwards, Tomas Mocek, and John Collier, "Kilowatt average power 100 J-level diode pumped solid state laser," Optica **4**, 438-439 (2017)

[2] Jonathan P. Phillips, Saumyabrata Banerjee, Jodie Smith, Mike Fitton, Tristan Davenne, Klaus Ertel, Paul Mason, Thomas Butcher, Mariastefania De Vido, Justin Greenhalgh, Chris Edwards, Cristina Hernandez-Gomez, and John Collier, "High energy, high repetition rate, second harmonic generation in large aperture DKDP, YCOB, and LBO crystals," Opt. Express **24**, 19682-19694 (2016)

[3] G. A. Mourou, G. Korn, W. Sandner, J. L. Collier, "Extreme Light Infrastructure—Whitebook, Science and Technology with Ultra-Intense Lasers", http://old.eli-beams.eu/wp-content/uploads/2011/10/ELI-Book_neues_Logo-edited-web.pdf

[4] K. Ertel, S. Banerjee, P. D. Mason, P. J. Phillips, M. Siebold, C. Hernandez-Gomez, and J. C. Collier, "Optimising the efficiency of pulsed diode pumped Yb:YAG laser amplifiers for ns pulse generation.," Opt. Express **19**, 26610-26626 (2011).

[5] J. Koerner, J. Hein, M. Kahle, H. Liebetrau, M. Lenski, M. Kaluza, M. Loeser, and M. Siebold, "Temperature dependent measurement of absorption and emission cross sections for various Yb3+ doped laser materials," Proc. SPIE **8080,** 808003 (2011).

[6] Cory Baumgarten, Michael Pedicone, Herman Bravo, Hanchen Wang, Liang Yin, Carmen S. Menoni, Jorge J. Rocca, and Brendan A. Reagan, "1 J, 0.5 kHz repetition rate picosecond laser," Opt. Lett. **41**, 3339-3342 (2016).

[7] Z. Bor, "Distortion of femtosecond laser pulses in lenses," Opt. Lett. **14**, 119-121 (1989).